Published in final edited form as:
Toxicology. 2012 May 16; 295(1-3): 56–67. doi:10.1016/j.tox.2012.01.017.

In utero exposure to benzo(a)pyrene predisposes offspring to cardiovascular dysfunction in later-life

Jules G.E.[a], **S. Pratap**[b], **A. Ramesh**[c], and **D.B. Hood**[a,*]

D.B. Hood: dhood@mmc.edu

[a]Department of Neuroscience and Pharmacology, Environmental-Health Disparities and Medicine, Center for Molecular and Behavioral Neuroscience, Meharry Medical College, Nashville, TN 37208, USA

[b]Department of Microbiology & Immunology, Microarray/Bioinformatics Core, Meharry Medical College, Nashville, TN 37208, USA

[c]Department of Biochemistry and Cancer Biology, Meharry Medical College, Nashville, TN 37208, USA

Abstract

In utero exposure of the fetus to benzo(a)pyrene [B(a)P], a polycyclic aromatic hydrocarbon, is thought to dysregulate cardiovascular development. To investigate the effects of *in utero* B(a)P exposure on cardiovascular development, timed-pregnant Long Evans Hooded (LEH) rats were exposed to diluent or B(a)P (150, 300, 600 and 1200 μg/kg/BW) by oral gavage on embryonic (E) days E14 (the metamorphosing embryo stage) through E17 (the 1st fetal stage). There were no significant effects of *in utero* exposure to B(a)P on the number of pups born per litter or in pre-weaning growth curves. Pre-weaning profiles for B(a)P metabolite generation from cardiovascular tissue were shown to be dose-dependent and elimination of these metabolites was shown to be time-dependent in exposed offspring. Systolic blood pressure on postnatal day P53 in the middle and high exposure groups of offspring were significantly elevated as compared to controls. Microarray and quantitative real-time PCR results were directly relevant to a biological process pathway in animal models for “regulation of blood pressure”. Microarray and quantitative real-time PCR analysis revealed upregulation of mRNA expression for angiotensin (AngII), angiotensinogen (AGT) and endothelial nitric oxide synthase (eNOS) in exposed offspring. Biological network analysis and gene set enrichment analysis subsequently identified potential signaling mechanisms and molecular pathways that might explain the elevated systolic blood pressures observed in B(a)P-exposed offspring. Our findings suggest that *in utero* exposure to B(a)P predispose offspring to functional deficits in cardiovascular development that may contribute to cardiovascular dysfunction in later life.

Keywords

Benzo(a)pyrene; Angiotensin; Microarray; Cardiovascular diseases; Hypertension; Susceptibility-exposure paradigm

Corresponding author. Tel.: +1 615 327 6358; fax: +1 615 327 6632.

Conflict of interest statement: None.

1. Introduction

The fetal origins of adult disease hypothesis proposes that coronary heart disease and stroke, and the disorders related to them, (*i.e.* hypertension and type 2 diabetes) originate through responses to under-nutrition during fetal life and infancy, which permanently change the body's structure and function in ways that lead to disease in later life (Barker, 1995). Experimental studies have also shown that manipulation of the diets of pregnant dams leads to life-long alterations in blood pressure and metabolism of their offspring (Hales et al., 1996; Barker, 2000). Further, there is a literature of longitudinal studies demonstrating that people born with low birth weight suffer from higher rates of stroke (Martyn et al., 1996; Eriksson et al., 2000; Rich-Edwards et al., 1997). Currently, very little is known about the mechanisms by which *in utero* insult leads to altered expression of key genes and proteins during early-life to result in diseased phenotypes in later-life. On the basis of epidemiology data in support of the Barker hypothesis, it is proposed that exposure to certain environmental chemicals as well as altered nutrition, or in combination with altered nutrition, will in some instances, not lead to readily discernable structural malformations but instead, to alterations in developmental programming expressed as a permanently altered gland, organ, or system potential. These effects will occur in a time-specific (*i.e.* vulnerable window) and tissue-specific manner, and such alterations maybe irreversible (Heindel, 2005).The later-life result is an animal that is sensitized such that it will be more susceptible to diseases later in life.

As a member of the polycyclic aromatic hydrocarbon (PAH) family, benzo(a)pyrene [B(a)P], is ubiquitous throughout the environment and is derived from the incomplete combustion of organic matter (Ramesh et al., 2011). Humans are exposed to PAHs through several routes that include air, water, food, skin contact and occupational settings. For a major portion of the general population that is not exposed to PAHs *via* proximity to sources of pollution or occupational modality, food ingestion is the major route of exposure as compared to inhalation (Butler et al., 1993). Previous studies on exposure of humans to B(a)P, have revealed that the range and magnitude of dietary exposures (2–500 ng/day) are exceedingly larger than for inhalation (10–50 ng/day) (Lioy et al., 1988) making exposure *via* diet a major route of exposure for PAHs (Beckman et al., 1998; Phillips, 1999).

PAH intake from ambient air has been reported to be in the range of 0.02–3 μg/day (World Health Organization, 2003). However, the levels vary depending on the geographic area, local traffic patterns, pollutant emissions from smokestacks, and personal habits such as smoking *etc.* In particular, occupational exposures to PAHs vary with the setting; 9.6–450 $\mu g/m^3$ in aluminum smelters, petroleum refineries, and copper mines. Occupational exposure to PAHs occurs in the production of aluminum, coal-fired power generating processes, iron and steel foundries, tar distillation, shale oil extraction, wood impregnation, roofing, road paving, carbon black production, carbon electrode production, restaurant cooking, diesel engine servicing, fire fighting, aviation fuel handling, chimney sweeping and calcium carbide production (Boffetta et al., 1997).

It is well established that environmental exposure to B(a)P can have multiple deleterious tissue effects depending on the dose, time (prenatal, postnatal) and term of exposure (for review see Ramesh et al., 2011). Because of the above mentioned considerations regarding potential routes of exposure, the present study sought to survey the health implications of *in utero* B(a)P exposure from the standpoint of developmental cardiovascular toxicity. The susceptibility-exposure paradigm utilized in this animal models study uses doses of B(a)P that may be perceived to be rather high. This is due to the fact that if doses that approximate ambient levels which humans are exposed were employed, we would seldom discern any manifestations of disease. It is within this context that it must be noted that the body/tissue

burden of aromatic hydrocarbons is governed by the daily intake doses, duration of exposure, and the half-life of this toxicant in the body (Grassman et al., 1998). The half-life of PAHs is greater in humans than in rodent tissues (National Academy of Sciences, 1983; Grassman et al., 1998). Furthermore, humans enjoy longer lifespan (about 30-fold longer) than rodents (Kim, 2007). If the interspecies differences in exposure history and toxicant accumulation characteristics are factored into experimental design, employing B(a)P doses higher than ambient levels is obligatory towards assessing the environmental health effects from exposure. Further, the B(a)P doses that we used in our study are of relevance to special B(a)P exposure scenarios in humans, which include cumulative intake from consumption of a B(a)P-contaminated diet, inhalation of tobacco smoke (both mainstream and side stream), breathing of contaminated air released from occupational settings (workers from petrochemical, graphite electrode and aluminum manufacturing industries), people/children that live in unvented homes using biomass for cooking and home heating and/or that work and play in the vicinity of hazardous waste sites (reviewed in WHO, 2010; Ramesh et al., 2010). Moreover, a recent review by our group reported on the global distribution of PAHs and detailed substantial environmental contamination (mg/g dry media or g/L water) by these toxicants (Ramesh et al., 2011). Therefore, it is our opinion that the cumulative annual intake of B(a)P by vulnerable and susceptible populations likely approximates the high B(a)P doses used in the present study.

Previous studies have reported that chronic exposure (12–24 weeks) of Apo-E knockout mice to 5 mg/kg B(a)P accelerated atherosclerotic plaques (Curfs et al., 2004). Also, a correlation was reported by these authors relative to the stages of plaques, reactive metabolites of B(a)P and formation of DNA adducts. This type of B(a)P exposure-induced atherosclerosis has been shown to be mediated through altered expression of antioxidant enzymes and enhanced generation of reactive oxygen species (ROS) in this mouse model (Yang et al., 2009). An enhanced expression of aryl hydrocarbon receptor (AhR) receptor target gene expression was also observed in mouse aortic endothelial cells suggesting that upregulation of AhR and of its target genes play a key role in B(a)P-induced atherogenesis (Wang et al., 2009).

Recent studies suggest that the pathogenic role of B(a)P may be attributed to its ability to be metabolized into highly reactive compounds, such as 6-hydroxy-B(a)P. These metabolites arise from the biological oxidation by mixed-function oxidases and the rapid autoxidation of 6-hydroxy-B(a)P to produce high levels of quinones and diones (Burdick et al., 2003b; Lorentzen and Ts'o, 1977; Lorentzen et al., 1979). These three groups of metabolites undergo one electron redox cycling (from quinone to semiquinone radical to hydroquinone forms) to generate large quantities of intracellular ROS (Burdick et al., 2003a; Flowers et al., 1996; Penning et al., 1996). The presence of two ROS species, such as hydrogen peroxide and superoxide anion, in turn react to form an even more reactive species, the hydroxyl radical. The presence of high levels of B(a)P metabolites combined with ROS produces a robust oxidative microenvironment that has been shown to cause DNA modifications and alterations in multiple cellular signaling pathways (Lorentzen et al., 1979).

Studies demonstrate that B(a)P is readily metabolized by the placenta and accumulates in fetal tissue during gestation (Bouayed et al., 2009). Likewise, recent studies also suggest that B(a)P adversely affects a number of fetal developmental indices such as low birth weight (Perera et al., 1998,1999,2003), impaired learning and memory (Perera et al., 2007, 2009), and decreased immune response (Hannah et al., 1982). Increasing evidence strongly suggests that B(a)P plays both a direct and indirect role in the development and progression of cardiovascular diseases (Gentner and Weber, 2011). Cardio- and cerebro-vascular events are more common in individuals with hypertension, hyperlipidemia, and diabetes mellitus,

and in smokers (Thirman et al., 1994). It has been well established that B(a)P, upon activation, is converted into a number of highly reactive intermediates that can bind to and modify DNA and protein structures (Miller and Ramos, 2001; Uno et al., 2004). These metabolites can also induce the production of reactive oxygen species which can damage the endothelium lining of blood vessels where macrophages and lipoproteins infiltrate and accumulate, to later form atherosclerotic lesions and plaques (Thirman et al., 1994). Numerous studies also suggest that cigarette smokers have a greater incidence and degree of atherosclerotic lesions (Thirman et al., 1994; Zhang and Ramos, 2008) however the specific biological and developmental pathways altered by *in utero* B(a)P exposure are poorly understood.

In the current study we examined the *in utero* effects of B(a)P exposure on gene expression in rat offspring heart tissue subsequent to *in utero* exposure to B(a)P. The results demonstrate that systolic blood pressure was significantly elevated. eNOS protein expression and mRNA levels for angiotensin (AngII) were also significantly increased in B(a)P exposed offspring compared to controls. Analysis of gene transcription microarray data revealed that 563 of the 16,000 genes were significantly altered in B(a)P-exposed offspring. Of the genes demonstrating modulation by B(a)P exposure, 377 genes were up-regulated greater than two-fold and 186 were down-regulated greater than two-fold. Common gene responses modulated as a result of B(a)P-exposure were identified and included xenobiotic metabolizing genes, genes known to alter lipid metabolism, nucleic acid metabolism, and more importantly, cardiovascular development and function. Among the most significantly altered pathways was the renin–angiotensin system pathway, with the angiotensinogen (AGT) gene demonstrating significant up-regulation as a result of *in utero* B(a)P exposure.

2. Materials and methods

2.1. Animals

To determine the total number of Long–Evans hooded dams (litters) as well as the number of offspring needed for these studies, we made the following assumptions. We conservatively estimated that the variance between measures from litters would be approximately 10% of the mean response, so that using littermates from four to five different litters within an experimental group would be sufficient to detect a significant difference. Based on these assumptions, the power analysis indicated that 3 replicates or cohorts from 4 to 5 different litters would suffice. Since the litter is the statistical unit and sampling was from at least 4 to 5 individual litters within an experimental group, the litter representation would be sufficient to detect a 20% change in any of our experimental end-points with an 80% power and a type-I error rate of 5%.

All experiments were approved by the Institutional Animal Care and Use Committee (IACUC) of Meharry Medical College (MMC) and were performed according to Guidelines for Animal Experimentation as set forth by the NIH. Timed-pregnant Long–Evans Hooded dams were obtained from Harlan Sprague–Dawley (St. Louis, MO, USA) on gestational day (GD) 11. Upon arrival, animals were housed individually in clear plastic cages with laboratory grade (heat-treated) pine shavings as bedding. Animals were quarantined for 2 days in the AAALAC = accredited MMC animal care facility and were maintained in a controlled environment with a temperature of 21 ± 2°C and relative humidity of 50–10% with a 12/12h light/dark cycle. Dams were fed commercial Rat Chow (#5012: Purina Mills, St. Louis, MO, USA), and water and food were available *ad libitum*.

2.2. Susceptibility-exposure paradigm and embryology from embryonic (E) days 14–17

Each dam was randomly assigned to either (1) control or (2) experimental group, and on E14–17 timed-pregnant dams were exposed by oral gavage using our susceptibility-exposure paradigm (Brown et al., 2007). E14 is known as the metamorphosing embryo stage where somites 43–45 (caudal); mandibular, maxillary, and frontonasal processes; cervical sinuses closing; mammary welts; differentiaion of handplates; arm buds vascularized, brachial nerves entering; beginning of umbilical hernia. On E17 or the 1st fetal stage, there is rapid growth of eyelids; palate completes; pinna covers ear ducts and the umbilical hernia withdraws.

Each dam was randomly assigned to either a (1) control or (2) experimental group, and on GD14–17 timed-pregnant dams were exposed by oral gavage using our susceptibility-exposure paradigm (Brown et al., 2007). Dams were given a total volume of 0.875 ml of (1) peanut oil alone or (2) 150,300,600 and 1200 μg/kg B(a)P in peanut oil. Offspring from control and B(a)P-exposed animals were maintained in standard stainless steel cages on pelleted paper bedding (#7084: Harlan, TX) until postnatal day P53, at which time they were sacrificed using previously described procedures (Sheng et al., 2010).

2.3. Tissue preparation and B(a)P disposition analysis

The connective tissue which partitions the aorta from the muscle of the thoracic cavity was dissected out. The epicardial and pericardial fat surrounding the heart and perivascular fat surrounding the aorta were also removed with fine tweezers. The aorta was cut above the point it emerges from the ventricular tissue. After heart and aorta were retrieved from the animal, organs and tissue were placed in a glass petridish and kept on ice. A small incision was made to the heart and whole blood was carefully drained from the heart and aorta into a heparinized conical tube. Washes proceeded with chilled isotonic saline at least 2 times to remove excess blood following which; the residual organ (heart plus aorta) was cut into small pieces using a sterile scalpel blade. Subsequently, the resulting samples of dissected cardiac tissues were minced separately with a fine pair of scissors, thoroughly mixed and then pooled per experimental group (n = 4–5/group/cohort) as a homogenate of minced, mixed and pooled tissue sample per experimental group and stored at −70°C until analyzed. Plasma from blood samples was harvested by centrifugation at 2900 × g for 20 min and stored frozen at −70°C until analyzed.

Prior to analyses, the plasma and heart-aorta samples were thawed and homogenized in 0.25 M Tris-sucrose-EDTA (pH 7.4) and 0.1% SDS. The homogenate was extracted with a solution containing water, methanol, and chloroform at a ratio of 1:1.5:2 (v/v). The organic phase was dried under N2 and resuspended in 0.5 ml of methanol. Particulates in the extracts were removed by passing them through Acrodisc filters (0.45 μm, 25-mm diameter; Gelman Sciences, Ann Arbor, MI, USA). The final extracts were stored at 4°C in amber-colored screwtop vials to prevent photodegradation until analysis. The bioavailable concentrations of metabolites from the extracts were identified and measured by a reverse-phase HPLC (Model 1200; Agilent, Wilmington, DE) equipped with a UV and a fluorescence detector as described previously (Brown et al., 2007).

B(a)P disposition analysis in plasma and whole heart-aorta tissue from control and B(a)P-exposed offspring was analyzed for bioavailable levels of B(a)P metabolites by liquid-liquid extraction and reverse phase high performance liquid chromatography (HPLC) as previously outlined in (Brown et al., 2007). Data were derived from 4 to 5 offspring per litter per group so that analyses represent repetitions from 3-cohorts comprising 12–15 offspring.

2.4. Blood pressure measurements

To assess whether *in utero* B(a)P exposure affected blood pressure in offspring rats, the systolic blood pressure of conscious-nonanesthetized animals (n = 5–6/litter/group) was measured on P53. Blood pressure was measured (noninvasive) by determining the tail blood volume with a volume pressure recording sensor and an occlusion tail-cuff (CODA System, Kent Scientific, Torrington, CT, USA). Windaq Acquisition 1.58 and Windaq Analysis 2.29 software (DATAQ Instruments DI200AC) were used to record and analyze the data, respectively. Briefly, offspring were conditioned restraint tubes from P46 through P50 prior to blood pressure measurements in the laboratory in which measurements were done. Analysis was performed two rats at a time by placed offspring in restraining tubes followed by tail cuff placement on tails. The Windaq Acquisition software was then set to perform a number of acclimatization runs to help condition the rats for the blood pressure measurement. After this acclimatization session, animals were returned to their home-cages in the animal care facility.

Regarding the potential for exposure to mild stress during the acclimatization session and during data acquisition; studies support the proposition that LEH rats adapt more readily to acute stress following prolonged exposure to a variety of mild stressors as compared to SD rats (Bielajew et al., 2002).

2.5. SDS-PAGE and Western blot analysis

Frozen samples of pooled heart tissue (described above in Section 2.2) from control and B(a)P-exposed offspring was thawed and homogenized in 1 ml RIPA buffer (Bio-Rad, USA) containing a protease-phosphatase inhibitor cocktail (Bio-rad, USA) for 1 min. Lysates were then centrifuged at 15000 RPM for 10 min, and the supernatant transferred to new tubes. Protein concentrations of the tissue lysates were determined using Bio-Rad protein assay reagent. Using 10% SDS-polyacrylamide gels, equal amounts of protein (from P-0 and P-53) were resolved under reducing conditions. Following electrophoresis the proteins were trans-blotted to Immobilon-FL membranes (Millipore Corporation, Billerica, MA, USA). Non-specific binding sites were blocked with 4% non-fat dry milk for 1.5 h and then incubated overnight at 4°C in polyclonal primary antibody against eNOS, nNOS or AngII (Santa Cruz, USA), with non-fat dry milk in Tris-buffered saline-Tween 20 buffer, while gently shaken. Next, the membranes were washed 4 times for 5 min each at room temperature in PBS + 0.1% Tween 20 with gentle shaking, using a generous amount of buffer. After washing, the membranes were incubated with a fluorescent secondary antibody raised against the primary antibody in non-fat dry milk in Tris-buffered saline + SDS +Tween 20. This incubation lasted for 1-h, after which the membranes were washed 4 × 5-min at room temperature with PBS + 0.1% Tween 20. Proteins were visualized and analyzed using the LiCor system.

2.6. RNA extraction

Total RNA was isolated from rat heart tissue with TRIzol reagent as described in accordance with the protocol suggested by the manufacturer (Life Technologies, Carlsbad, CA, USA). RNA was purified using an mRNA purification kit from Promega (Madison WI, USA).

2.7. Quantitative real time RT-PCR

Three genes known to be involved in blood pressure regulation (AngII, nNOS and eNOS) were selected to be measured by qRT-PCR. Additionally, (BH4/BH2) oxi-doreductase (Spr) was also quantified. Quantitative Real time RT-PCR was carried out using the iScript one-step RT-PCR kit with SYBR Green, PCR plates and optically clear adhesive plate seals (Bio-Rad Laboratories, USA). A Bio-Rad C1000 Thermal Cycler was used to detect the

fluorescence level. Reactions were carried out in low 96-well clear PCR plates, with a 2 × PCR buffer containing 0.4 mM of each dNTP (dATP, dCTP, dGTP, dTTP), SYBR Green dye, magnesium ions, 20 nM fluorescein, iTaq DNA Polymerase and stabilizers. Forward and reverse primers (300 nM final concentration each), nuclease-free water, RNA template (1 pg-100ng total RNA) and iScript reverse transcriptase for one-step RT-PCR were added to PCR buffer in a final reaction volume of 50 μl. Amplification parameters were: cDNA synthesis at 50°C for 10 min, followed by reverse transcriptase inactivation at 95°C for 5 min, PCR cycling and detection (30–45 cycles) at 95°C for 30s; and 55–60°C at 30s (data collection step). All primers were designed using OligoPerfect Designer Software (Invitrogen, USA) and can be found in Table 1. Samples were analyzed in duplicate, and 18 S rRNA primers were used (Ambion, Austin, TX, USA) as the endogenous control. Fold induction was calculated using the formula $2^{-\Delta\Delta CT}$, where ΔC_T = target gene C_T – actin C_T, and the $\Delta\Delta C_T$ is based on the mean ΔC_T of respective control [non-B(a)P treated]. The C_T value is determined as the cycle at which the fluorescence signal emitted is significantly above background levels and is inversely proportional to the initial template copy number.

2.8. cDNA microarray hybridization, data acquisition and analysis

For this study, RNA samples were extracted from heart tissue and submitted to the Vanderbilt Functional Genomics Shared Resource facility (FGSR). All RNA samples processed in the Vanderbilt FGSR were checked on the Agilent 2100 Bio-analyzer to determine integrity, and quantitated by A260 on the Thermo Nanodrop 2000 spectrophotometer. Samples with a minimum RNA Integrity Number (RIN) score of 7.0 and with 260/280 ratio of 1.9–2.1 were used in microarray experiments. The Agilent 1-color Low Input Quick Amp (LIQA) target labeling kit and Agilent 1-color spike-in were used to prepare targets for hybridization following the manufacturer's protocols. Briefly, 100 ng input total RNA was mixed with diluted RNA spike-ins per protocol specifications. The target reactions were reverse transcribed, and then the reverse transcription products were used in transcription reactions according to the manufacturer's protocol using the Agilent QuickAmp kit. The Cy labeled cRNA targets were quantitated and specific activity of each labeled target was calculated. All yields ranged from 6.0 to 8.5 μg, with specific activity ranging from 19 to 22 across the 8 reactions. Minimum requirements for hybridization are 1.65 μg of cRNA target and specific activity greater than 6.0. Equivalent mass of each co-hybridized sample (0.825 μg) was combined, fragmented, and then placed in hybridization cocktail. Smear assessments of the cRNA target all had a majority of the target between 200 and 2000 nt (recommendation for smear assessment is a majority of target between 200 and 2000 nt). A total of 70% or more of each target fell within this size range. Targets were fragmented for 30s at 60°C and then 2 × Hi-RPM Buffer was added. Hybridizations were set up at 65°C, 10RPM, for 17-h hybridization in an Agilent Hybridization chamber. Hybridizations were taken down and washed per Agilent protocol. The arrays were scanned on the Agilent “C” scanner at 3 μm, 20bit. Next, 2, 4 × 44k 1 color Gene Expression slides were run on the Agilent “C” using the recommended settings of 3 μm resolution, 20 bit pixel depth. The gain used was G 100%. Data were processed using Feature Extraction 10.7.1, and analyzed with GE1_107_Sep09 FE protocol. The data were then analyzed by gene set enrichment analysis for statistically significant overexpressed pathways. The WEBGESTALT software tool was used to conduct enrichment analysis by mapping transcripts which were up or down-regulated greater than 2-fold to their corresponding reference Kyoto Encyclopedia of Genes and Genomes (KEGG) pathways and Gene Ontology (GO) biological process pathways (Zhang et al., 2005). An interaction network visualization of GO biological processes was created using the GeneMANIA plug in (Mostafavi et al., 2008) for the Cytoscape bioinformatics platform (Shannon et al., 2003).

2.9. Statistical analysis

B(a)P metabolite levels, systolic blood pressure and heart rate data are expressed as mean ± SEM. The cardiac function values of each animal were obtained through the average of 15 values (each value collected at 1-min intervals during the 30-min experimental period). Statistical significance was estimated using 2-way ANOVA followed by the Bonferroni post test. The level of significance was set at $p < 0.05$ (GraphPad Prism 5.0). The values for eNOS, nNOS, AngII and 7,8-dihydrobiopterin (BH4/BH2) oxidoreductase (Spr) mRNA and/or protein are reported as means ± SEM. An analysis of variance (ANOVA) was used for the determination of statistical differences between control and B(a)P-exposed offspring groups All pairwise multiple comparisons were performed using the Student-Newman-Keuls method. The criterion for statistical significance was $p < 0.05$ in all cases.

2.10. RNA-extraction

Tissue samples destined for RNA analysis were lysed with Trizol reagent and RNA extracted according to the manufacturer's instructions. The RNA pellet was dissolved in nuclease-free water and subjected to clean-up using RNeasy columns (Qiagen, Hilden, Germany) with on-column DNase treatment for the removal of genomic DNA.

RNA quality and integrity were assessed using the Nanodrop spectrophotometer (Nanodrop Technologies, Montchanin, USA) and 2100 Bioanalyzer (Agilent Technologies, Waldbronn, Germany) respectively. Samples with ratios of absorbance at 280/260 nm between 1.8 and 2.0 and at 280/230 nm between 2.0 and 2.2, and with RNA integrity number (RIN) of ≥ 7.5 were judged to be of acceptable quality and integrity to be used for microarray labelling.

2.10.1. RNA isolation and reverse transcription-real time quantitative PCR assay (RT-qPCR)—Total RNA isolated as described above using the TRIzol method (Invitrogen, Cergy-Pontoise, France) was then reverse-transcribed into cDNA using the RT Applied Biosystems kit (Foster City, CA). qPCR assays were performed next using the fluorescent dye SYBR Green methodology and an ABI Prism 7300 detector (Applied Biosystems). The gene specific primers were provided by Qiagen (Courtaboeuf, France). The specificity of each gene amplification was verified at the end of qPCR reactions through analysis of dissociation curves of the PCR products. Amplification curves were analysed with ABI Prism 7000 SDS software using the comparative cycle threshold method. Relative quantification of the steady-state target mRNA levels was calculated after normalization of the total amount of cDNA tested to 18 S mRNA endogenous reference. Target gene mRNA expression is presented as the relative fold change between the intensity of the target-specific band to that of the 18sRNA band on P53 as compared to P0 in both control and B(a)P-exposed offspring (600 and 1200 μ/kg BW). An analysis of variance (ANOVA) was used for the determination of statistical differences between control and B(a)P-exposed offspring groups All pairwise multiple comparisons were performed using the Student–Newman–Keuls method. The criterion for statistical significance was $p < 0.05$ in all cases.

2.11. Determination of 7,8-dihydrobiopterin (BH4/BH2) oxidoreductase (Spr) mRNA levels

In order to determine the potential for whether increasing BH4 concentrations precipitate endothelial dysfunction in offspring rats subsequent to *in utero* B(a)P exposure, assessment was performed by RT-PCR for determination of BH4 precursor sepiapterin (BH2) by monitoring 7,8-dihydrobiopterin:NADP+ oxidoreductase also known as sepiapterin reductase, (Spr). Total RNA was isolated as described above. Forward primer for 7,8-dihydrobiopterin (BH4/BH2) oxidoreductase (Spr) was 5′-ACAGCCCATCTCTGAGTGC-3′ and reverse primer 5′-CTTCATAATGGCCTCCA-3′.

3. Results

3.1. Toxicological observations

Consistent with previous reports (Baldwin et al., 2005; Brown et al., 2007) as well as from our group (Wu et al., 2003; Wormley et al., 2004), there were no significant differences in the number of pups born per litter between control and B(a)P-exposed dams (Table 2). Likewise, no convulsions, tremors, abnormal movements or any other predictable or reproductive indicators of toxicity were observed during the exposure or pre-weaning period in any of the five treatment groups of offspring.

3.2. In utero B(a)P exposure has no effect on total body weight of rat offspring

At the various postnatal days (P0, 3, 5, 7, 9, 11 and 13), offspring were removed from each control or B(a)P treatment groups. Total body weight was measured for each offspring. Offspring were then anesthetized and sacrificed, at which point whole blood was harvested subsequent to cardiac puncture. As depicted in Fig. 1, the there were no significant differences between the total body weights in control and B(a)P-exposed offspring for any of the pre-weaning time points.

3.3. In utero B(a)P exposure results in metabolite disposition in rat offspring

To confirm whether B(a)P was absorbed into the blood for metabolism and distributed to target tissues, a bioavailability study was conducted during the pre-weaning period (P0–13)using plasma and heart tissue from exposed offspring. Timed-pregnant dams were exposed to diluent (control) or various concentrations of B(a)P *in utero* on E14 to E17 (0,150,300, 600 and 1200 μg/kg BW respectively). The data obtained in Fig. 2A and B demonstrate that offspring from the B(a)P-exposed groups exhibit dose-dependent disposition of total B(a)P metabolites in both plasma (Fig. 2A) and whole heart tissue, respectively (Fig. 2B). A time-dependent decrease in total B(a)P metabolites was also documented during the pre-weaning period.

As indicated in Fig. 2C, there were three principal groups of metabolite types (diols, hydroxy derivatives and diones). The percent distribution of diol metabolites was high throughout the preweaning period and remained over 70% of the total heart tissue burden. On the other hand, the hydroxyl B(a)P metabolites increased in distribution between P9 and P13, while the diones remained fairly constant in their distribution from P0 to P13. The qualitative distribution of total B(a)P metabolites depicted in Fig. 2C suggest that both phase 1 and phase 2 (toxification and detoxification) pathways were activated within exposed offspring plasma and heart tissue. The sustained presence of the hydroxy derivatives within heart tissue is of even greater significance, as these highly reactive metabolites can be further oxidized into quinones, which have the potential to undergo redox cycling to form more reactive oxygen species (ROS) (Baldwin et al., 2005; Brown et al., 2007; Zhang et al., 2005). In summary, B(a)P metabolite concentrations and metabolite types in heart tissues quantified in the present study were found to be in agreement with those detected in developing rodent brain tissues as previously reported (Brown et al., 2007; McCallister et al., 2008; Sheng et al., 2010).

3.4. In utero B(a)P exposure increases systolic blood pressure in a dose-dependent manner in rat offspring

To determine whether *in utero* B(a)P exposure results in alterations in later-life cardiovascular phenotypes, offspring were analyzed for heart rate, systolic and diastolic blood pressure. These parameters were measured on P53. The results are shown as Table 3B. The results shown in Table 3B and Fig. 3, demonstrate that *in utero* B(a)P exposure induced a statistical significant increase in heart rate, systolic and diastolic blood pressure in

a dose-dependent manner in exposed offspring. Control systolic blood pressure averaged 131.5 ± 5.8 mmHg. Systolic blood pressure in offspring from the 600 μg/kg BW B(a)P group indicated a small, but statistically significant increase (19% higher than controls), while offspring in the 1200 μg/kg BW B(a)P showed an even greater increase in systolic blood pressure as compared to controls (53% higher than controls).

3.5. In utero exposure to B(a)P upregulates eNOS protein in offspring

As a means of determining whether the observed increase in systolic blood pressure was related to alterations in the renin–angiotensin system, heart tissue proteins critical to this system were quantified using Western blot analysis. The results shown in Fig. 4 illustrate that temporal developmental expression of eNOS from B(a)P-exposed offspring cardiac tissue is positively modulated as a result of *in utero* B(a)P exposure. In control offspring, eNOS expression is high during the first postnatal week and drops to presumably constitutive levels from P10 through P53. In exposed offspring, it is readily apparent that there is an overall dose-dependent increase in developmental eNOS expression. Modulation of developmental eNOS expression as a result of *in utero* exposure to B(a)P (when compared to controls) is evidenced by very low expression during the first postnatal week followed by an increase in expression through P 53for the 600 μg/kg BW B(a)P-exposed offspring. This overall upregulation of developmental expression appears to be dose-dependent as developmental expression is further potentiated in the 1200 μg/kg BW B(a)P-exposed offspring (Fig. 4).

3.6. In utero B(a)P exposure upregulates eNOS, nNOS, AngII and 7,8-dihydrobiopterin (BH4/BH2) oxidoreductase (Spr) mRNA levels in offspring

In order to corroborate the overall developmental protein expression data obtained, qRT-PCR was performed for Ang II, eNOS, nNOS and dihydrobiopterin oxidoreductase mRNAs.The fold change in relative mRNA levels was greater for nNOS and AGT at 600 μg/kg BW B(a)P on PND 53. Fig. 6 shows the corroboration data for the results shown as Fig. 5. The fold change in relative mRNA levels is greater for nNOS and AngII at 600 μg/kg BW B(a)P on P53. Consistent with the developmental protein expression profiling data in Fig. 5, eNOS mRNA expression is 2.8 fold above control levels in the 1200 μg/kg BW B(a)P-exposed offspring on P53 with AngII mRNA expression at 1.75 fold above control levels. The key observation of these experiments comes with analysis of 7,8-dihydrobiopterin NADP oxidoreductase or BH4/BH2 oxidoreductase mRNA expression in the 1200 μg/kg BW B(a)P-exposed offspring on P53 in comparison to the other data epochs. That the BH4/BH2 oxidoreductase and eNOS mRNA are upregulated in comparison to the other experimental groups is significant and suggest that early-life B(a)P exposure results in later-life eNOS uncoupling. This hypothesis is presented in the discussion section.

3.7. Transcriptome microarray pathway enrichment analysis

The results from the transcriptome microarray were analyzed by gene set enrichment analysis for statistically significant over-expressed pathways in a comparison of control *versus* exposed offspring [1200 μg/kg BW B(a)P]. The WEBGESTALT software tool was used to map transcripts which were up or down-regulated greater than 2 fold to their corresponding reference Kyoto Encyclopedia of Genes and Genomes (KEGG) pathways (Zhang et al., 2005). A hypergeometric test with a Benjamini–Hochburg (BH) false discovery rate correction was used to determine significantly enriched KEGG pathways. The results are shown in Table 3A. As would be expected, a number of CYPs in exposed heart tissue were modulated as a result of *in utero* exposure to B(a)P. The genes identified were CYP2a2, CYP7a1 and CYP2b12.

Of note is significant enrichment in the renin–angiotensin system pathway (KEGG pathway: rno04614). AGT among other genes involved in blood pressure regulation, was shown to be differentially expressed in the microarray and suggest that this modulation is a result of *in utero* exposure to B(a)P. The results are directly relevant to a biological process pathway in animal models for "regulation of blood pressure". Further, we see this as an attempt to put these results into perspective with respect to the gene ontology literature in cardiovascular toxicology. In this modality, Angiotensin (AngII) was set as a seed gene in order to build an interaction and co-expression network of associated genes in Rat offspring using the GeneMANIA plug in and the Cytoscape bioinformatics platform.

4. Discussion

To the best of our knowledge, this is the first report of its kind showing that *in utero* B(a)P exposure from E14-E17 results in functional cardiovascular deficits in later life. Reports in the literature demonstrate that the daily exposure of humans to B(a)P ranges from μg to mg levels (reviewed in Dutta et al., 2010). The debate regarding the high doses of B(a)P used in our studies becomes a bit more palatable upon critically analyzing the literature in the area germane to "fetal basis of PAH-induced deficits in different experimental model systems." (spanning from toxicity to cancer)" This review reveals that a range of concentrations have been utilized. The concentrations used in the present study are well within the range of B(a)P concentrations represented in these very important seminal studies that have defined systemic toxicity.

Illustrative of this fact, pregnant C57 mice when gavaged with 100 or 500 μg/kg BW/day B(a)P on embryonic days 10–13 showed dysmorphogenesis of renal tubules and progressive loss of renal function at postnatal weeks 7 and 52 in the offspring (Nanez et al, 2011). In a representative high dose study, B6129F1 mice when gavaged with 1000 or 15,000 μg/kg BW/day di-methyl benzan-thracine (DMBA) on embryonic day 17 revealed lung adenomas and carcinomas in offspring, that also exhibited significant mortalities between postnatal weeks 10 and 30 (Castro et al, 2008). Prior to this report, when C57 mice were subcutaneously administered 1000 μg DMBA or B(a)P/kg BW/week for 3-weeks prior to pregnancy, the ovarian reserve in offspring was reduced by 1/3 as compared to unexposed control mice (Jurisicova et al., 2007). We offer these seminal studies to demonstrate the range of B(a)P exposure doses utilized in "differential experimental model systems" that were employed to interrogate hypothesis germane to "fetal basis of PAH-induced deficits in animal models." The doses employed in the present study fall well within the range of the doses employed in the above-mentioned studies. Further, the toxic effects reported in the present study reinforce the notion that early-life, *in utero* exposure to PAHs results in a diverse spectrum of pathophysiological changes that are transmitted and expressed during later-life in the offspring.

In the present study, *in utero* exposure resulted in altered gene expression of both Angiotensinogen (AGT) and AngII, potentially predisposing the offspring to the development of hypertension. Although similar studies have been done using a similar exposure paradigm in mice (Thackaberry et al., 2005; Aragon et al., 2008a,b) the AhR agonist used (*i.e.* 2, 3, 7, 8-tetrachlorodibenzo-[p]-dioxin(TCDD) was a much stronger agonist than B(a)P. However, the results from these studies clearly demonstrate that the environmental toxicant TCDD significantly altered genes involved in fetal cardiac homeostasis, cell cycle regulation, and extracellular matrix development and remodeling (Thackaberry et al., 2005). In addition, Aragon et al. (2008a,b) further demonstrated that most of the TCDD-induced changes in cardiac gene expression observed during fetal development remained induced in the adult mice, all of which probably further predispose the mice to cardiovascular dysfunction (Aragon et al., 2008a,b).

Very little is known of the long term effects of B(a)P on the development and function of the cardiovascular system of pre-natally exposed offspring. Endothelial dysfunction can be broadly defined as a disruption in any of the regulatory processes of the endothelium, including an imbalance between vasorelaxing and constricting factors leading to dysregulation of smooth muscle tone (Rubanyi, 1993). The AngII treatment of mice offspring exposed *in utero* and during lactation to TCDD, resulting in increased predisposition to renal fibrosis and hypertension in adulthood (Aragon et al., 2008a,b), clearly supports the findings in the present study. When AngII was infused during the pre-weaning period into TCDD exposed mice offspring, systolic blood pressure increased in a robust manner as compared to control offspring (Aragon et al., 2008a,b). These studies support the contention that the B(a)P exposure-induced increase in systolic blood pressure in the present study is likely mediated by the vasoconstricting factor, angiotensin II. In both human and animal models, hypertension is often associated with increased circulating angiotensin II (Kaplan, 2002).

In the present study, we demonstrated that B(a)P [an aryl hydrocarbon (AhR) receptor agonist] precipitates toxic effects within the developing cardiovascular system in our animal model. Previous studies have reported variations on this central theme (Aboutabl et al., 2009; Burstyn et al., 2005), and have even included other AhR agonists (Heid et al., 2001; Kang et al., 2006; Kopf et al., 2008; Korashy and El-Kadi, 2006). In humans, 2,3,7,8-tetrachlorodibenzo-[p]-dioxin (TCDD; a much more potent and stable AhR agonist than B(a)P) exposure was associated with cardiovascular diseases such as hypertension (Kang et al., 2006; Kim et al., 2003; Pesatori et al., 2003). Polychlorinated biphenyls, also AhR agonists, have been shown to cause endothelial dysfunction. This effect may be mediated by increased oxidative stress from AhR-induced CYP1A1 activity (Hennig et al., 2002; Ramadass et al., 2003).

There have been three previous studies conducted in animal models that have suggested that B(a)P exposure accelerates the development of atherosclerosis (Curfs et al., 2004; Penn and Snyder, 1988; Yang et al., 2009), and the present study provides further evidence that this may be attributable to increased oxidative stress. The identification of the developmental period over which there is formation/accumulation of the reactive 3-OH and 9-OH metabolites in the developing cardiovascular system is a key finding of this study. The identified B(a)P exposure-induced metabolites could further oxidize to form B(a)P quinones that would undergo redox cycling and generate reactive oxygen species (Kerzee and Ramos, 2000; Kiruthiga et al., 2007).

In support of our findings as to involvement of reactive oxygen species are the experiments in Fig. 5 demonstrating that eNOS and BH4/BH2 7,8-dihydrobiopterin NADP oxidoreductase or BH4/BH2 oxidoreductase mRNA is upregulated in offspring from the high dose group. Collectively our data supports the proposed mechanism that is presented as Fig. 7. Recall that dihydrobiopterin and/or tetrahydrobiopterin serve as critical co-factors for the endothelial nitric-oxide synthase (eNOS). Deficiency of BH4/BH2 results in eNOS uncoupling that is associated with increased superoxide and decreased $NO^{\bullet}$ production (Kuzkaya et al., 2003). BH4 has been shown to play a critical role in allowing for electron transfer from the prosthetic heme to l-arginine (Kuzkaya et al., 2003). In the absence of BH4, electron flow from the reductase domain to the oxygenase domain is diverted to molecular oxygen rather than to l-arginine, leading to a condition known as eNOS uncoupling (Xia et al., 1998; Radi et al., 1991), causing production of superoxide rather than nitric oxide. Superoxide reacts rapidly with $NO^{\bullet}$ to form the peroxynitrite anion ($ONOO^{-}$), which is a strong biological oxidant (Sampson et al., 1996) known to oxidize lipids, protein, sulfhydryls, and DNA and to cause nitration of tyrosines (Sampson et al., 1996; Zhao et al., 2001; Daiber and Ullrich, 2002).

Supplementation with BH4 is generally able to restore endothelial NO synthase (eNOS)-mediated NO formation and endothelial function in hypertension, hypercholesterol-emia and diabetes (Alp and Channon, 2004; Cosentino and Luscher, 1999; Vasquez-Vivar et al., 2002). It is well known that nitric oxide (NO) generated by eNOS critically determines vascular tone as well as vascular wall homeostasis (Fleming and Busse, 2003). Reduced NO bioavailability then has been associated with an increase in the formation of reactive oxygen species within the vascular wall and generally serves as the key determinant of endothelial dysfunction (Bauersachs and Schafer, 2005). This phenomenon was demonstrated by Cai et al. (2005) who showed reduced eNOS dimer/monomer ratio in combination with increased oxidative stress and reduced NO formation in hyperglycaemic endothelial cells (Table 4).

The paradoxical finding of a concomitant increase in eNOS expression and reduced endothelium-dependent vasodilatation/relaxation by Bouloumié et al. (1997), Bauersachs et al. (1999) and Cosentino et al. (1997) has drawn attention to the fact that eNOS itself in pathological states maybe the source of superoxide anions, *i.e.* “eNOS uncoupling” (for review, see Stuehr et al., 2001). Endothelial dysfunction and eNOS uncoupling are clearly apparent in experimental diabetes and in diabetic patients (Guzik et al., 2002; Hink et al., 2001) despite the fact that eNOS expression is actually increased (Bauersachs and Schafer, 2005). The uncoupling of eNOS has also been linked to its monomerization (Zou et al., 2002).

Similarly, in Apo E knock-out mice, peroxynitrite-mediated BH4 oxidation has also been identified as a pathogenic cause of eNOS uncoupling (Laursen et al., 2001). It is safe to say that numerous common diseases such as hypercholesterolemia, hypertension, diabetes, and heart failure are associated with a loss of $NO^{\bullet}$ production by the endothelium, a condition commonly referred to as endothelial dysfunction (Zeiher et al., 1993). In many of these conditions, eNOS uncoupling seems to be present, leading to an increase in endothelial cell $O_2^{\bullet -}$ production and a decrease in $NO^{\bullet}$ production (Kuzkaya et al., 2003). In the present study, the results suggest eNOS uncoupling mediated by 7,8-dihydrobiopterin NADP oxidoreductase (BH4/BH2) mRNA upregulation to result in (1) decreased nitric oxide production (NO), (2) increased superoxide radical ($O_2^{\bullet -}$) and (3) peroxynitrite anion (ONOO−). The effect of introducing oxidative B(a)P-metabolites into this cycle upregulates the expression of the BH4/BH2 oxidoreductase as was empirically determined in Fig. 5. These three scenarios are proposed to lead to the apparent later-life (P53) uncoupling of eNOS as a result of high oxidative cardiovascular tissue burdens during early-life, developmental processes.

Additionally, PAHs are also known to cause adverse inflammatory effects in the respiratory system (Borm et al., 1997). B(a)P and other AhR agonists increase the expression of proinflammatory cytokines such as interleukin-8 and tumor necrosis factor-alpha (TNF-α) which in turn cause infiltration of macrophages and neutrophils into the lung (Borm et al., 1997; Podechard et al., 2008). Not only do activated pulmonary neutrophils cause increased ROS but they also may act synergistically with pulmonary B(a)P to produce an even larger number of reactive B(a)P metabolites than would be produced in the absence of pulmonary neutrophils (Borm et al., 1997). Further, inflammatory cytokines, once produced, circulate systemically causing increased production of oxygen free radicals in distal tissues including vascular smooth muscle cells (De Keulenaer et al., 1998). Future work will focus on characterizing possible relationships between inflammatory mediators and PAH reactive metabolites serving as a source of oxidative stress leading to increased NO bioactivity in the peripheral vasculature to result in later-life cardiovascular diseased phenotypes in offspring.

It remains a daunting challenge to link exposure to components of air pollution during development with later-life alterations in cardiovascular disease phenotypes. The present

study is most informed by the genome-wide analyses of aryl hydrocarbon receptor (AhR) agonist effects on gene clusters (Sartor et al., 2009). The study by Sartor and colleagues has provided important information regarding the potential for dysregulation of potential operative pathways. The study found that the AhR in unstimulated cells binds to an extensive array of gene clusters with functions in the regulation of gene expression, differentiation and pattern specification, thereby connecting multiple morphogenetic and developmental programs. The global network that was identified constituted a critical new resource for the study of AhR-regulated gene expression that should prompt new hypotheses to promote a more comprehensive understanding of the physiological role of the AhR and of the resulting deleterious health effects from exposure of the human population to environmental AhR agonists.

5. Conclusion

Exposure to polycyclic aromatic hydrocarbons during embryonic life may derail the concerted expression of genes critical to normal cardiovascular system development to alter the normal patterns of expression of these genes. The resulting altered phenotype likely persists throughout life and contributes to the determination of disease susceptibility in the adult. Future studies from our laboratory will explore the possibility of epigenetic modifications in offspring tissues subsequent to *in utero* B(a)P-exposure.

Acknowledgments

Special thanks to our colleagues Michael G. Izban, Ph.D. for assistance with RNA preparation analyses and Diana Marver, Ph.D. for critical review of the manuscript.

Funding: This work was supported, in part, by NIH grants S11ES014156-05, U54NS041071-002, 1R56ES017448-01A1 and 3P20 MD000516-07S1 to D.B.H.; 1R01CA142845-01A1 to A.R. Also, critical to the conduct of these studies were grants from the Simons Foundation Autism Research Initiative, Research Centers in Minority Institutions (RCMI) grant G12RRO3032, Nuclear Regulatory Commission Grant NRC-27-10-515 and Meharry Medical College-Vanderbilt University Alliance for Research Training in Neuroscience Grant (T32MH065782).

References

Aboutabl ME, Zordoky BN, El-Kadi AO. 3-Methylcholanthrene and benzo(a)pyrene modulate cardiac cytochrome P450 gene expression and arachidonic acid metabolism in male Sprague Dawley rats. Br J Pharmacol. 2009; 158(7):1808–1819. [PubMed: 19889059]

Alp N, Channon KM. Regulation of endothelial nitric oxide synthase by tetrahydrobiopterin in vascular disease. Arterioscler Thromb Vasc Biol. 2004; 24:413–420. [PubMed: 14656731]

Aragon A, Goens M, Carbett E, Walker M. Perinatal 2,3,7,8-tetrachlorodibenzo-p-dioxin exposure sensitizes offspring to angiotensin II-induced hypertension. Cardiovasc Toxicol. 2008a; 8(3):145–154. [PubMed: 18670907]

Aragon AC, Kopf PG, Campen MJ, Huwe JK, Walker MK. In utero and lactational 2,3,7,8-tetrachlorodibenzo-p-dioxin exposure: effects on fetal and adult cardiac gene expression and adult cardiac and renal morphology. Toxicol Sci. 2008b; 101(2):321–330. [PubMed: 17975115]

Baldwin NE, Chesler EJ, Kirov S, Langston MA, Snoddy JR, Williams RW, Zhang B. Computational, integrative, and comparative methods for the elucidation of genetic coexpression networks. J Biomed Biotechnol. 2005; 2005(2):172–180. [PubMed: 16046823]

Barker, DJP. Fetal Origins of Cardiovascular and Lung Disease. RCOG Press; New York, NY: 2000.

Barker DJP. Fetal origins of coronary heart disease. BMJ. 1995; 311:171–174. [PubMed: 7613432]

Bauersachs J, Bouloumié A, Fraccarollo D, Hu K, Busse R, Ertl G. Endothelial dysfunction in chronic myocardial infarction despite increased vascular endothelial nitric oxide synthase and soluble guanylyl cyclase expression: role of enhanced vascular superoxide production. Circulation. 1999; 100:292–298. [PubMed: 10411855]

Bauersachs J, Schafer A. Tetrahydrobiopterin and eNOS dimer/monomer ratio-a clue to eNOS uncoupling in diabetes? Cardiovasc Res. 2005; 65(4):768–769. [PubMed: 15721855]

Beckman, SO.; Thuvander, A.; Andersson, C. Preview of PAHs in Food: Potential Health Effects and Contents in Food. Vol. 8. National Food Administration; Uppsala, Sweden: 1998.

Bielajew C, Konkle ATM, Merali Z. The effects of chronic mild stress on male Sprague-Dawley and Long–Evans rats I. Biochem Physiol Anal. 2002; 136:583–592.

Boffetta P, Jourenkova N, Gustavsson P. Cancer risk from occupational and environmental exposure to polycyclic aromatic hydrocarbons. Cancer Causes Control. 1997; 8(3):444–472. [PubMed: 9498904]

Borm PJ, Knaapen AM, Schins RP, Godschalk RW, Schooten FJ. Neutrophils amplify the formation of DNA adducts by benzo[a]pyrene in lung target cells. Environ Health Perspect. 1997; 105(Suppl. 5):1089–1093. [PubMed: 9400705]

Bouayed J, Desor F, Rammal H, Kiemer AK, Tybl E, Schroeder H, Rychen G, Soulimani R. Effects of lactational exposure to benzo[alpha]pyrene (B[alpha]P) on postnatal neurodevelopment, neuronal receptorgene expression and behaviour in mice. Toxicology. 2009; 259(3):97–106. [PubMed: 19428949]

Bouloumié A, Bauersachs J, Linz W, Schflkens B, Wiemer G, Fleming I. Endothelial dysfunction coincides with an enhanced NO synthase expression and superoxide anion production. Hypertension. 1997; 30:934–941. [PubMed: 9336396]

Brown LA, Khousbouei H, Goodwin JS, Irvin-Wilson CV, Ramesh A, Sheng L, McCallister MM, Jiang GC, Aschner M, Hood DB. Down-regulation of early ionotrophic glutamate receptor subunit developmental expression as a mechanism for observed plasticity deficits following gestational exposure to benzo(a)pyrene. Neurotoxicology. 2007; 28(5):965–978. [PubMed: 17606297]

Burdick AD, Davis JW, Liu II, Hudson KJ, Shi LG, Monske H, Burchiel MLSW. Benzo(a)pyrene quinones increase cell proliferation, generate reactive oxygen species, and transactivate the epidermal growth factor receptor in breast epithelial cells. Cancer Res. 2003a; 63:7825–7833. [PubMed: 14633709]

Burdick AD, Davis JW, Liu KJ, Hudson LG, Shi H, Monske ML, Burchiel SW. Benzo(a)pyrene quinones increase cell proliferation, generate reactive oxygen species, and transactivate the epidermal growth factor receptor in breast epithelial cells. Cancer Res. 2003b; 63(22):7825–7833. [PubMed: 14633709]

Burstyn I, Kromhout H, Partanen T, Svane O, Langard S, Ahrens W, Kaup-pinen T, Stucker I, Shaham J, Heederik D, Ferro G, Heikkila P, Hooiveld M, Johansen C, Randem B, Boffetta P. Polycyclic aromatic hydrocarbons and fatal ischemic heart disease. Epidemiology. 2005; 16(6):744–750. [PubMed: 16222163]

Butler J, Post G, Lioy P, Waldman J, Greenberg A. Assessment of carcinogenic risk from personal exposure to benzo(a)pyrene in the total human environmental exposure study. J Air Waste Manage Assoc. 1993; 43(7):970–977.

Castro DJ, Baird WM, Pereira CB, Giovanini J, Lohr CV, Fischer KA, Yu Z, Gonzalez FJ, Krueger SK, Williams DE. Fetal mouse Cyp1b1 and transplacental carcinogenesis from maternal exposure to dibenzo(a,l)pyrene. Cancer Prevent Res. 2008; 1(2):128–134.

Cai S, Khoo J, Channon KM. Augmented BH4 by gene transfer restores nitric oxide synthase function in hyperglycemic human endothelial cells. Cardiovasc Res. 2005; 65:823–831. [PubMed: 15721862]

Cosentino F, Hishikawa K, Katusic Z, Luscher TF. High glucose increases nitric oxide synthase expression and superoxide anion generation in human aortic endothelial cells. Circulation. 1997; 96:25–28. [PubMed: 9236411]

Cosentino F, Luscher TF. Tetrahydrobiopterin and endothelial nitric oxide synthase activity. Cardiovasc Res. 1999; 43:274–278. [PubMed: 10536654]

Curfs DM, Lutgens E, Gijbels MJ, Kockx MM, Daemen MJ, Van Schooten FJ. Chronic exposure to the carcinogenic compound benzo[a]pyrene induces larger and phenotypically different atherosclerotic plaques in ApoE-knockout mice. Am J Pathol. 2004; 164(1):101–108. [PubMed: 14695324]

Daiber A, Ullrich V. Peroxynitrite reactions with heme and heme-thiolate (P450) proteins. Methods Enzymol. 2002; 359:379–389. [PubMed: 12481588]

De Keulenaer GW, Alexander RW, Ushio-Fukai M, Ishizaka N, Griendling KK. Tumour necrosis factor alpha activates a p22phox-based NADH oxidase in vascular smooth muscle. Biochem J. 1998; 329(Pt 3):653–657. [PubMed: 9445395]

Dutta K, Ghosh D, Nazmi A, Kumawat KL, Basu A. A common carcinogen benzo[a]pyrene causes neuronal death in mouse via microglial activation. PLoS ONE. 2010; 5(4):e9984. [PubMed: 20376308]

Eriksson J, Forsen T, Tuomilehto J, Osmond C, Barker D. Early growth, adult income and risk of stroke. Stroke. 2000; 31:869–874. [PubMed: 10753990]

Fleming I, Busse R. Molecular mechanisms involved in the regulation of the endothelial nitric oxide synthase. Am J Physiol Regul Integr Comp Physiol. 2003; 284:R1–R12. [PubMed: 12482742]

Flowers L, Bleczinski WF, Burczynski ME, Harvey RG, Penning TM. Disposition and biological activity of benzo[a]pyrene-7,8-dione. A geno-toxic metabolite generated by dihydrodiol dehydrogenase. Biochemistry. 1996; 35:13664–13672. [PubMed: 8885846]

Gentner NJ, Weber LP. Intranasal benzo[a]pyrene alters circadian blood pressure patterns and causes lung inflammation in rats. Arch Toxicol. 2011; 85:337–346. [PubMed: 20848083]

Grassman JA, Masten SA, Walker NJ, Lucier GW. Animal models of human response to dioxins. Environ Health Perspect. 1998; 106(Suppl. 2):761–775. [PubMed: 9599728]

Guzik T, Mussa S, Gastaldi D, Sadowski J, Ratnatunga C, Pillai R. Mechanisms of increased vascular superoxide production in human diabetes mellitus: role of NAD(P)H oxidase and endothelial nitric oxide synthase. Circulation. 2002; 105:1656–1662. [PubMed: 11940543]

Hales C, Desai M, Ozanne S, Crowther NJ. Fishing in the stream of diabetes: from measuring insulin to the control of fetal organogenesis. Biochem Soc Trans. 1996; 24:341–350. [PubMed: 8736760]

Hannah JB, Hose JE, Landolt ML, Miller BS, Felton SP, Iwaoka WT. Benzo(a)pyrene-induced morphologic and developmental abnormalities in rainbow trout. Arch Environ Contam Toxicol. 1982; 11(6):727–734. [PubMed: 6819818]

Heid SE, Walker MK, Swanson HI. Correlation of cardiotoxicity mediated by halogenated aromatic hydrocarbons to aryl hydrocarbon receptor activation. Toxicol Sci. 2001; 61(1):187–196. [PubMed: 11294989]

Heindel JJ. The fetal basis of adult disease: role of environmental exposures–introduction. Birth Defects Res A: Clin Mol Teratol. 2005; 73:131–132. [PubMed: 15751038]

Hennig B, Meerarani P, Slim R, Toborek M, Daugherty A, Silverstone AE, Robertson LW. Proinflammatory properties of coplanar PCBs: in vitro and in vivo evidence. Toxicol Appl Pharmacol. 2002; 181(3):174–183. [PubMed: 12079426]

Hink U, Li H, Mollnau H, Oelze M, Matheis E, Hartmann M. Mechanisms underlying endothelial dysfunction in diabetes mellitus. Circ Res. 2001; 88:e14–e22. [PubMed: 11157681]

Jurisicova A, Taniuchi A, Li H, Shang Y, Antenos M, Detmar J, Xu J, Matikainen T, Ito Hernandez A, Nunez G, Casper RF. Maternal exposure to poly-cyclic aromatic hydrocarbons diminishes murine ovarian reserve via induction of Harakiri. J Clin Invest. 2007; 117(12):3971–3978. [PubMed: 18037991]

Kang HJ, Kim HJ, Kim SK, Barouki R, Cho CH, Khanna KK, Rosen EM, Bae I. BRCA1 modulates xenobiotic stress-inducible gene expression by interacting with ARNT in human breast cancer cells. J Biol Chem. 2006; 281(21):14654–14662. [PubMed: 16567799]

Kaplan N. Hypertension and diabetes. J Hum Hypertens. 2002; 16(Suppl. 1):S56–S60. [PubMed: 11986896]

Kerzee JK, Ramos KS. Activation of c-Ha-ras by benzo(a)pyrene in vascular smooth muscle cells involves redox stress and aryl hydrocarbon receptor. Mol Pharmacol. 2000; 58(1):152–158. [PubMed: 10860937]

Kim JS, Lim HS, Cho SI, Cheong HK, Lim MK. Impact of Agent Orange exposure among Korean Vietnam veterans. Ind Health. 2003; 41:149–157. [PubMed: 12916744]

Kim SK. Common aging pathways in worms, flies, mice and humans. J Exp Biol. 2007; 210:1607–1612. [PubMed: 17449826]

Kiruthiga PV, Shafreen RB, Pandian SK, Arun S, Govindu S, Devi KP. Protective effect of silymarin on erythrocyte haemolysate against benzo(a)pyrene and exogenous reactive oxygen species (H2 O2) induced oxidative stress. Chemosphere. 2007; 68(8):1511–1518. [PubMed: 17481694]

Kopf P, Huwe J, Walker M. Hypertension, cardiac hypertrophy, and impaired vascular relaxation induced by 2,3,7,8-tetrachlorodibenzo-p-dioxin are associated with increased superoxide. Cardiovasc Toxicol. 2008; 8(4):181–193. [PubMed: 18850075]

Korashy HM, El-Kadi AOS. The role of aryl hydrocarbon receptor in the pathogenesis of cardiovascular diseases. Drug Metab Rev. 2006; 38(3):411–450. [PubMed: 16877260]

Kuzkaya N, Weissmann N, Harrison D, Dikalov S. Interactions of peroxynitrite, tetrahydrobiopterin, ascorbic acid, and thiols: implications for uncoupling endothelial nitric-oxide synthase. J Biol Chem. 2003; 278(25):22546–22554. [PubMed: 12692136]

Laursen J, Somers M, Kurz S, McCann L, Warnholtz A, Freeman BA. Endothelial regulation of vasomotion in apoE-deficient mice: implications for interactions between peroxynitrite and tetrahydrobiopterin. Circulation. 2001; 103:1282–1288. [PubMed: 11238274]

Lioy P, Waldman J, Greenberg A, Harkov R, Pietarinen C. The Total Human Environmental Exposure Study (THEES) to benzo(a)pyrene: comparison of the inhalation and food pathways. Arch Environ Health. 1988; 43(4):304–312. [PubMed: 3415358]

Lorentzen RJ, Ts'o PO. Benzo[a]yrenedione/benzo[a]pyrenediol oxida-tionreduction couples and the generation of reactive reduced molecular oxygen. Biochemistry. 1977; 16:1467–1473. [PubMed: 191070]

Lorentzen RJ, Lesko SA, McDonald K, Ts'o POP. Toxicity of metabolic benzo(a)pyrenediones to cultured cells and the dependence upon molecular oxygen. Cancer Res. 1979; 39(8):3194–3198. [PubMed: 455303]

Martyn C, Barker D, Osmond C. Mothers' pelvic size, fetal growth, and death from stroke and coronary heart disease in men in the UK. Lancet. 1996; 348:1264–1268. [PubMed: 8909378]

McCallister MM, Maguire M, Ramesh A, Aimin Q, Liu S, Khoshbouei H, Aschner M, Ebner FF, Hood DB. Prenatal exposure to benzo(a)pyrene impairs later-life cortical neuronal function. Neurotoxicology. 2008; 29(5):846–854. [PubMed: 18761371]

Miller KP, Ramos KS. Impact of cellular metabolism on the biological effects of benzo(a)pyrene and related hydrocarbons. Drug Metab Rev. 2001; 33(1):1–35. [PubMed: 11270659]

Mostafavi S, Debajyoti R, Warde-farley D, Grouios C. GeneMANIA: a real-time multiple association network integration algorithm for predicting gene function. Genome Biol. 2008; S4(Suppl. 1):9.

Nanez A, Ramos IN, Ramos KS. A mutant *Ahr* allele protects the embryonic kidney from hydrocarbon-induced deficits in fetal programming. Environ Health Perspect. 2011; 119

National Academy of Sciences. Polycyclic Aromatic Hydrocarbons: Evaluation of Sources and Effects. Vol. 476. National Academy Press; Washington, DC: 1983.

Penn A, Snyder C. Arteriosclerotic plaque development is “promoted” by polynuclear aromatic hydrocarbons. Carcinogenesis. 1988; 9(12):2185–2189. [PubMed: 3142695]

Penning TM, Ohnishi ST, Ohnishi T, Harvey RG. Generation of reactive oxygen species during the enzymatic oxidation of polycyclic aromatic hydrocarbon trans-dihydrodiols catalyzed by dihydrodiol dehydrogenase. Chem Res Toxicol. 1996; 9:84–92. [PubMed: 8924621]

Perera FP, Jedrychowski W, Rauh V, Whyatt RM. Molecular epidemiologic research on the effects of environmental pollutants on the fetus. Environ Health Perspect. 1999; 107(Suppl. 3):451–460. [PubMed: 10346993]

Perera FP, Li Z, Whyatt R, Hoepner L, Wang S, Camann D, Rauh V. Prenatal airborne polycyclic aromatic hydrocarbon exposure and child IQ at age 5 years. Pediatrics. 2009; 124(2):e195–e202. [PubMed: 19620194]

Perera FP, Rauh V, Tsai WY, Kinney P, Camann D, Barr D, Bernert T, Garfinkel R, Tu YH, Diaz D, Dietrich J, Whyatt RM. Effects of transplacental exposure to environmental pollutants on birth outcomes in a multiethnic population. Environ Health Perspect. 2003; 111(2):201–205. [PubMed: 12573906]

Perera FP, Tang D, Rauh V, Tu YH, Tsai WY, Becker M, Stein JL, King J, Del PG, Lederman SA. Relationship between polycyclic aromatic hydrocarbon-DNA adducts, environmental tobacco

smoke, and child development in the World Trade Center cohort. Environ Health Perspect. 2007; 115(10):1497–1502. [PubMed: 17938742]

Perera FP, Whyatt RM, Jedrychowski W, Rauh V, Manchester D, Santella RM, Ottman R. Recent developments in molecular epidemiology: a study of the effects of environmental polycyclic aromatic hydrocarbons on birth outcomes in Poland. Am J Epidemiol. 1998; 147(3):309–314. [PubMed: 9482506]

Pesatori AC, Consonni D, Bachetti S, Zocchetti C, Bonzini M, Baccarelli A, Bertazzi PA. Short- and long-term morbidity and mortality in the population exposed to dioxin after the Seveso accident. Ind Health. 2003; 41(3):127. [PubMed: 12916742]

Phillips DH. Polycyclic aromatic hydrocarbons in the diet. Mut Res/Genet Toxicol Environ Mut. 1999; 443(1-2):139–147.

Podechard N, Lecureur V, Le Ferrec r, Guenon E, Sparfel I, Gilot L, Gordon D, Lagente JR, Fardel VO. Interleukin-8 induction by the environmental contaminant benzo(a)pyrene is aryl hydrocarbon receptor-dependent and leads to lung inflammation. Toxicol Lett. 2008; 177(2):130–137. [PubMed: 18289803]

Radi R, Beckman JS, Bush KM, Freeman BA. Peroxynitrite oxidation of sulfhydryls. The cytotoxic potential of superoxide and nitric oxide. J Biol Chem. 1991; 266:4244–4250. [PubMed: 1847917]

Ramadass P, Meerarani P, Toborek M, Robertson LW, Hennig B. Dietary flavonoids modulate PCB-induced oxidative stress CYP1A1 induction, and AhR-DNA binding activity in vascular endothelial cells. Toxicol Sci. 2003; 76(1):212–219. [PubMed: 12970578]

Ramesh A, Archibong A, Niaz MS. Ovarian susceptibility to benzo[a]pyrene: tissue burden of metabolites and DNA adducts in F-344 rats. J Toxicol Environ Health A. 2010; 73:1611–1625. [PubMed: 20967675]

Ramesh, A.; Archibong, AE.; Hood, DB.; Guo, Z.; Loganathan, BG. Global environmental distribution and human health effects of polycyclic aromatic hydrocarbons In: Global Contamination Trends of Persistent Organic Chemicals. CRC Press; Boca Raton: 2011. p. 95-124.

Rich-Edwards J, Stampfer M, Manson J, Rosner B, Hankinson S, Colditz G, Wil-lett W, Hennekens CH. Birth weight and risk of cardiovascular disease in a cohort of women followed up since 1976. BMJ. 1997; 315:396–400. [PubMed: 9277603]

Rubanyi GM. The role of endothelium in cardiovascular homeostasis and diseases. J Cardiovasc Pharmacol. 1993; 22(Suppl. 4):S1–S14. [PubMed: 7523767]

Sampson JB, Rosen H, Beckman JS. Peroxynitrite-dependent tyrosine nitration catalyzed by superoxide dismutase, myeloperoxidase, and horseradish peroxidase. Methods Enzymol. 1996; 269:210–218. [PubMed: 8791651]

Sartor M, Schnekenburger M, Marlowe J, Reichard J, Wang Y, Fan Y, Ma C, Karyala S, Halbleib D, Liu X, Medvedovic M, Puga A. Genomewide analysis of aryl hydrocarbon receptor binding targets reveals an extensive array of gene clusters that control morphogenetic and developmental programs. Environ Health Perspect. 2009; 117:1139–1146. [PubMed: 19654925]

Shannon P, Markiel A, Ozier O, Baliga NS, Wang JT, Ramage D, Amin N, Schwikowski B, Ideker T. Cytoscape: a software environment for integrated models of biomolecular interaction networks. Genome Res. 2003; 13:2498–2504. [PubMed: 14597658]

Sheng L, Ding X, Ferguson M, McCallister M, Rhoades R, Maguire M, Ramesh A, Aschner M, Campbell D, Levitt P, Hood DB. Prenatal polycyclic aromatic hydrocarbon exposure leads to behavioral deficits and downregulation of receptor tyrosine kinase. MET Toxicol Sci. 2010; 118(2):625–634.

Stuehr D, Pou S, Rosen GM. Oxygen reduction by nitric-oxide synthases. J Biol Chem. 2001; 276:14533–14536. [PubMed: 11279231]

Thackaberry EA, Jiang Z, Johnson CD, Ramos KS, Walker MK. Toxi-cogenomic profile of 2,3,7,8-tetrachlorodibenzo-p-dioxin in the murine fetal heart: modulation of cell cycle and extracellular matrix genes. Toxicol Sci. 2005; 88(1):231–241. [PubMed: 16120747]

Thirman MJ, Albrecht JH, Krueger MA, Erickson RR, Cherwitz DL, Park SS, Gelboin HV, Holtzman JL. Induction of cytochrome CYPIA1 and formation of toxic metabolites of benzo[a]pyrene by rat aorta: a possible role in atherogenesis. Proc Natl Acad Sci U S A. 1994; 91(12):5397–5401. [PubMed: 8202497]

Uno S, Dalton TP, Derkenne S, Curran CP, Miller ML, Shertzer HG, Nerbert DW. Oral exposure to benzo[a]pyrene in the mouse: detoxication by inducible cytochrome P450 is more important than metabolic activation. Mol Pharmacol. 2004; 65:1225–1237. [PubMed: 15102951]

Vasquez-Vivar J, Martasek P, Whitsett J, Joseph J, Kalyanaraman B. The ratio between tetrahydrobiopterin and oxidized tetrahydrobiopterin analogues controls superoxide release from endothelial nitric oxide synthase: an EPR spin trapping study. Biochem J. 2002; 362:733–739. [PubMed: 11879202]

Wang Z, Yang H, Ramesh A, Roberts II, Zhou LJ, Lin L, Zhao X, Guo YZ. Overexpression of Cu/Zn-superoxide dismutase and/or catalase accelerates benzo(a)pyrene detoxification by upregulation of the aryl hydrocarbon receptor in mouse endothelial cells. Free Radic Biol Med. 2009; 47(8):1221–1229. [PubMed: 19666105]

WHO. IARC Monographs on the Evaluation of the Carcinogenic Risks to Humans. Vol. 92. World Health Organization; Geneva, Switzerland: 2010. Some non-heterocyclic polycyclic aromatic hydrocarbons and some related exposures; p. 861

World Health Organization. Environmental Health Criteria 229. United Nations Environment Programme, the International Labour Organization and the World Health Organization; Geneva: 2003. Selected nitro- and nitro-oxy-polycyclic aromatic hydrocarbons.

Wormley DD, Chirwa S, Nayyar T, Wu J, Johnson S, Brown LA, Harris E, Hood DB. Inhaled benzo(a)pyrene impairs long-term potentiation in the F1 generation rat dentate gyrus. Cell Mol Biol (Noisy-le-grand). 2004; 50(6):715–721. [PubMed: 15641162]

Wu J, Ramesh A, Nayyar T, Hood DB. Assessment of metabolites and AhR and CYP1A1 mRNA expression subsequent to prenatal exposure to inhaled benzo(a)pyrene. Int J Dev Neurosci. 2003; 21(6):333–346. [PubMed: 12927582]

Xia Y, Tsai AL, Berka V, Zweier JL. Superoxide generation from endothelial nitric-oxide synthase. A Ca^{2+}/calmodulin-dependent and tetrahydrobiopterin regulatory process. J Biol Chem. 1998; 273:25804–25808. [PubMed: 9748253]

Yang H, Zhou L, Wang Z, Roberts II, Lin LJ, Zhao X, Guo YZ. Overexpression of antioxidant enzymes in ApoE-deficient mice suppresses benzo(a)pyrene-accelerated atherosclerosis. Atherosclerosis. 2009; 207(1):51–58. [PubMed: 19409565]

Zeiher AM, Drexler H, Saurbier B, Just H. Endothelium-mediated coronary blood flow modulation in humans. Effects of age, atherosclerosis, hypercholesterolemia, and hypertension. J Clin Invest. 1993; 92:652–662. [PubMed: 8349804]

Zhang B, Kirov S, Snoddy J. WebGestalt: an integrated system for exploring gene sets in various biological contexts. Nucleic Acids Res. 2005; 33(Web Server issue):W741–W748. [PubMed: 15980575]

Zhang Y, Ramos KS. The development of abdominal aortic aneurysms in mice is enhanced by benzo(a)pyrene. Vasc Health Risk Manag. 2008; 4(5):1095–1102. [PubMed: 19183758]

Zhao K, Whiteman M, Spencer JP, Halliwell B. DNA damage by nitrite and peroxynitrite: protection by dietary phenols. Methods Enzymol. 2001; 335:296–307. [PubMed: 11400378]

Zou M, Shi C, Cohen RA. Oxidation of the zinc-thiolate complex and uncoupling of endothelial nitric oxide synthase by peroxynitrite. J Clin Invest. 2002; 109:817–826. [PubMed: 11901190]

Abbreviations

PAHs	polycyclic aromatic hydrocarbons
B(a)P	benzo(a)pyrene
LEH	Long–Evans hooded
ED	embryonic day
P	postnatal day
ANGII	angiotensin

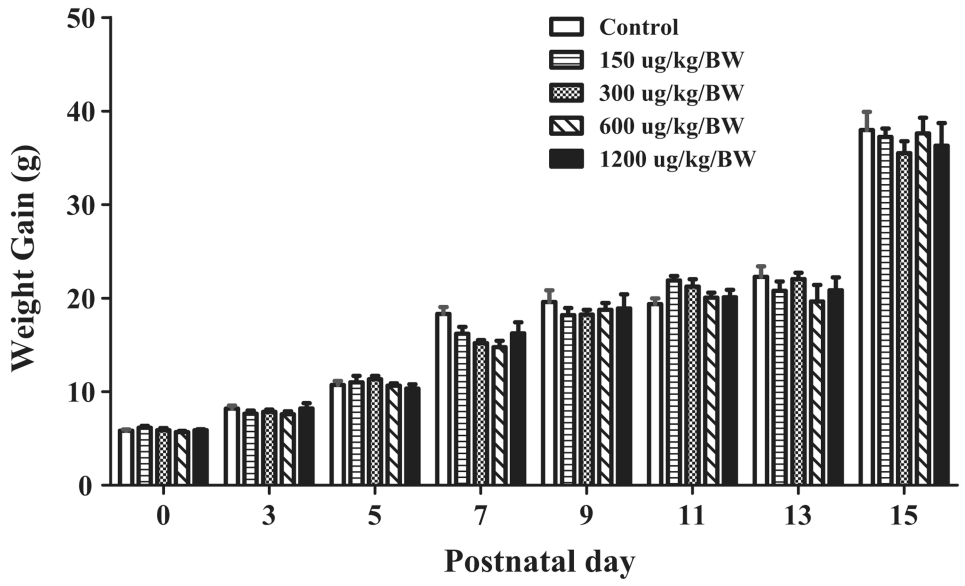

Fig. 1.

Absence of an *in utero* B(a)P-exposure effect on body weight in offspring. Offspring from dams exposed to different concentrations of B(a)P (0, 600 and 1200 μg/kg BW respectively) were sacrificed. Weights were measured prior to sacrifice. There were no significant difference between the controls and B(a)P-exposed offspring. Values are expressed as the mean ± SEM of three separate experiments in which weights were averaged from four to five rat offspring.

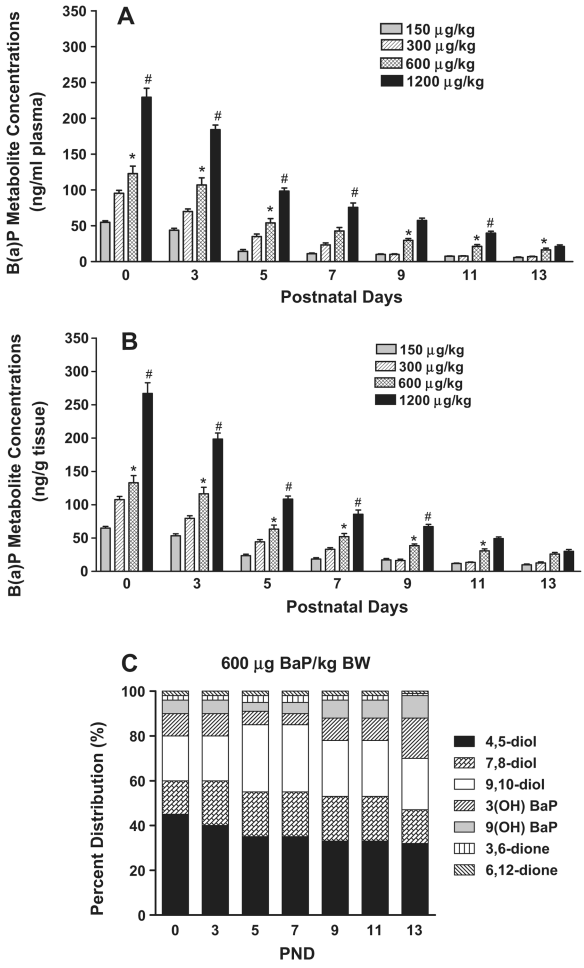

Fig. 2.

(A) The effect of *in utero* B(a)P exposure on metabolite disposition in offspring. Offspring from dams exposed to different concentrations of B(a)P (150, 300, 600 and 1200 μg/kg BW B(a)P respectively) were anesthetized and sacrificed. B(a)P metabolites were extracted from plasma (A) followed by HPLC analysis. Total B(a)P metabolites increased in a dose-dependent manner, and were eliminated in a time-dependent manner. Values are expressed as the mean ± SEM of three separate experiments in which plasma were pooled from three LEHR offspring. *p-value ≤0.05, $^{\#}p$-value ≤0.01 significantly different from 150 μg/kg BW B(a)P. (B) *In utero* B(a)P-exposure effects on metabolite disposition in developing cardiac tissue. Offspring from dams exposed to different concentrations of B(a)P (150, 300, 600 and 1200 μg/kg BW B(a)P respectively) were anesthetized and sacrificed. B(a)P metabolites were extracted from cardiac tissue (B) followed by HPLC analysis. Total B(a)P metabolites increased in a dose-dependent manner, and were eliminated in a time-dependent manner. Values are expressed as the mean ± SEM of three separate experiments in which hearts were pooled from three LEHR offspring. *p-value ≤0.05, $^{\#}p$-value ≤0.01 significantly different from 150 μg/kg BW B(a)P. (C) *in utero* B(a)P exposure affects the qualitative distribution of metabolites in offspring. Offspring from dams exposed to different concentrations of B(a)P(150,300,600 and 1200 μg/kg/BW B(a)P respectively) were anesthetized and sacrificed. The percentage distribution of B(a)P metabolites found in hearts of B(a)P-exposed offspring is shown in Fig. 3C. The data shown is a representative sample of 600 μg/kg BW B(a)P.

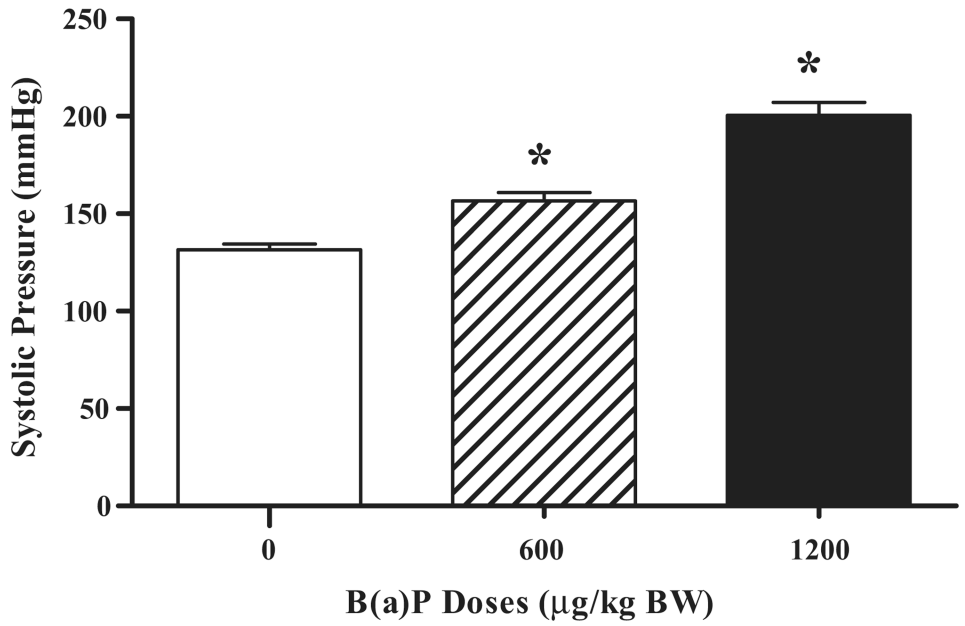

Fig. 3.

In utero B(a)P-exposure negatively affects systolic blood pressure in offspring. The blood pressure of offspring from dams exposed to different concentrations of B(a)P(0,600 and 1200 μg/kg BW respectively) were measured using tail cuff (Kent Scientific, USA). Each session consisted of 5 acclimatization cycles followed by 15 BP measurements cycles. A set was accepted if the computer identified >50% successful readings. Values are expressed as the mean ± SEM of three separate experiments in which blood pressure measurements were averaged from four-five rat offspring.

**p*-value ≤0.05 significantly different from control.

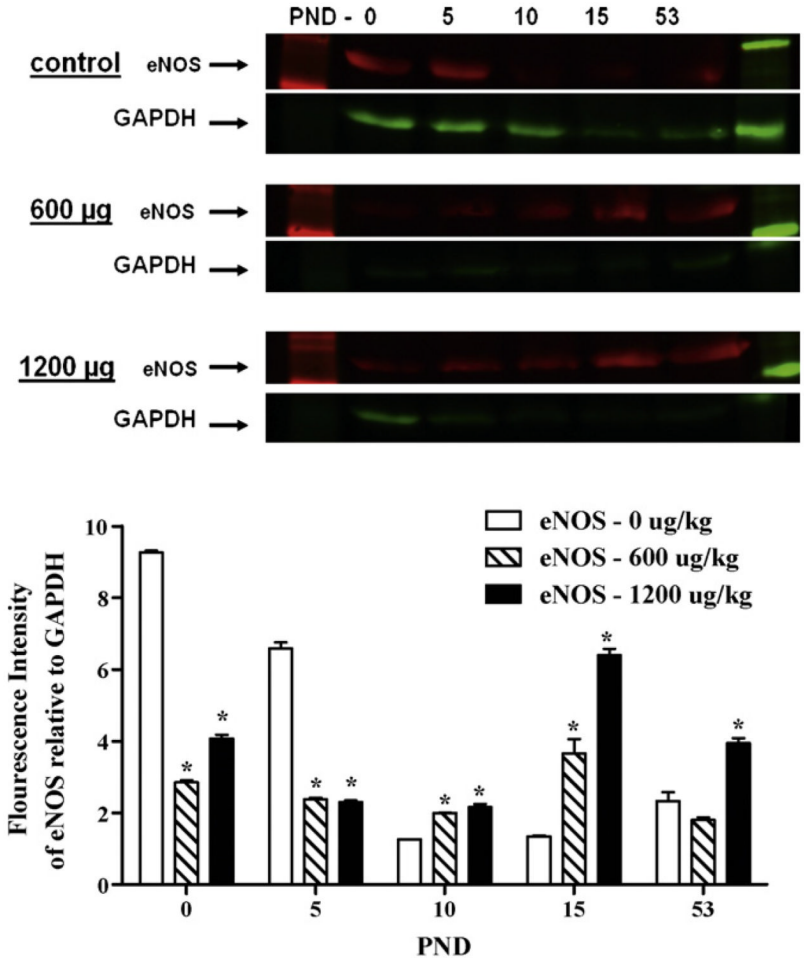

Fig. 4.

In utero B(a)P-exposure upregulates cardiac tissue eNOS protein expression in offspring. Offspring from dams exposed to different concentrations of B(a)P (150, 300, 600 and 1200 μg/kg/BW B(a)P respectively) were anesthetized, sacrificed and major organs collected. Protein lysates were extracted from cardiac tissue for treatment groups 0, 600 and 1200 μg/kg BW respectively, for P-0, -5, -10, -15 and -53. Lysates protein concentration were determined and then analyzed by western blot. The data shown is a representative sample of three gels (see figure). The bands depict immunocomplexes for eNOS and the internal control, GAPDH, at P-0, -5,-10,-15 and -53.

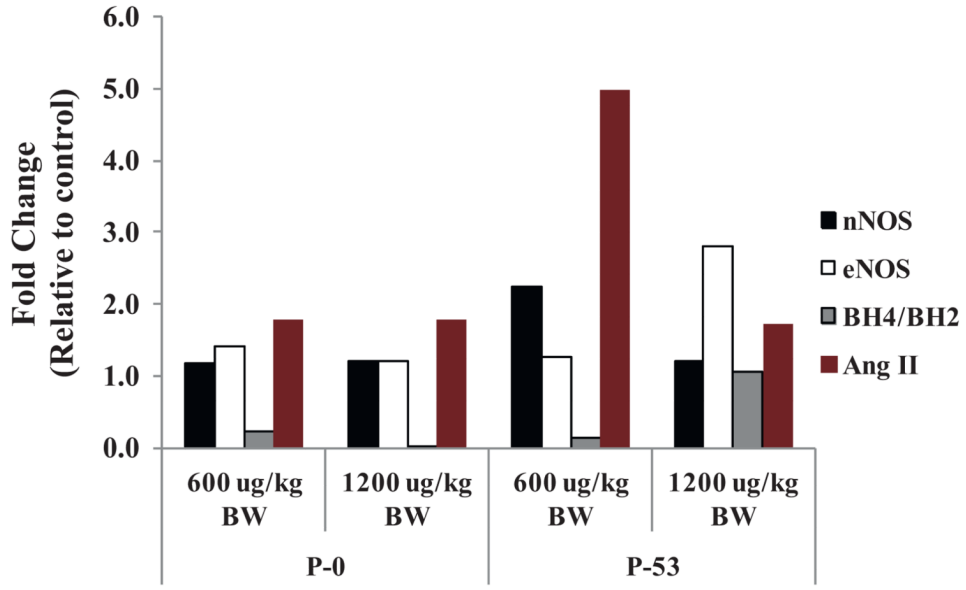

Fig. 5.

In utero B(a)P-exposure upregulates heart nNOS, eNOS, BH4/BH2 oxidore-ductase and AngII mRNA in offspring. Relative expression levels of nNOS, eNOS, BH4/BH2 and AngII as measured by qRT-PCR. Quantitative RT-PCR was performed using iScript one-step RT-PCR kit with SYBR Green, PCR plates, optically clear adhesive plate seals (Bio-Rad Laboratories, USA), and RNA template from offspring exposed *in utero* to different concentrations of B(a)P (0, 600 and 1200 μg/kg BW respectively). The mRNA expression levels were determined using primers purchased from Invitrogen (USA). A Bio-Rad C1000 Thermal Cycler was used to detect the fluorescence level. Relative expression was calculated using the formula $2^{-\Delta\Delta C_T}$. All relative mRNA values were normalized to 18S rRNA levels.

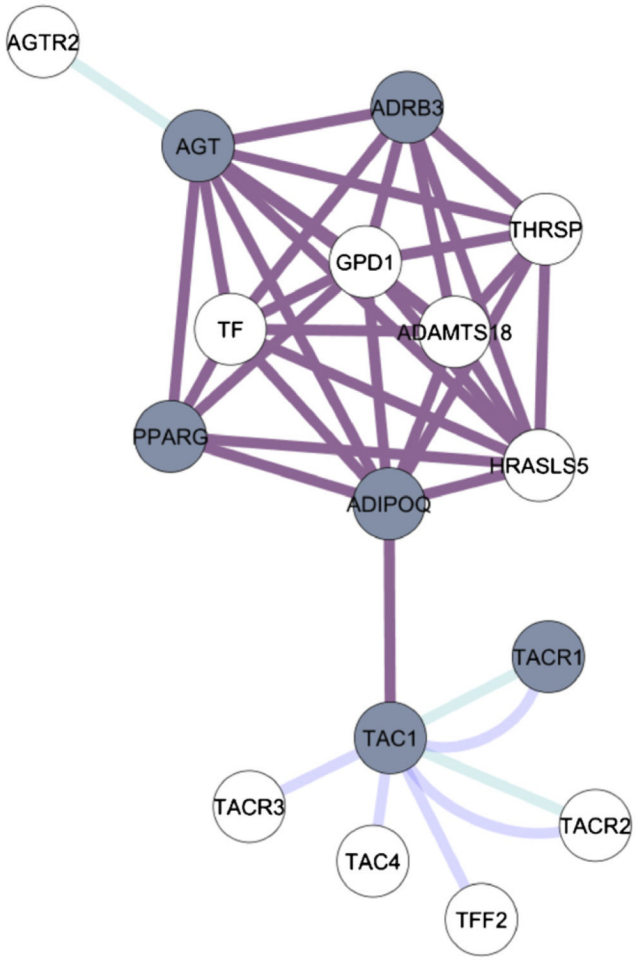

Fig. 6.

The effect of *in utero* B(a)P-exposure on genes in the "Regulation of Blood Pressure" Gene Ontology biological processed (GO:008217) in LEH rat offspring. Angiotensin (AGT) was set as a seed gene in order to build an interaction and co-expression network of associated genes in Rat using the GeneMANIA plug-in and the Cytoscape bioinformatics platform. Nodes in grey had greaterthan 2-fold expression differences (up or down-regulation) in the microarray dataset.

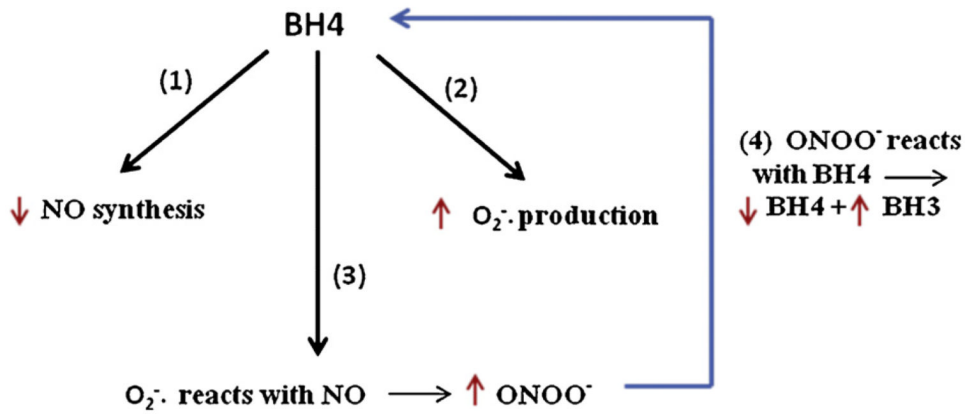

Fig. 7.

Proposed Mechanism for Endothelial Dysfunction. 7,8-dihydrobiopterin NADP oxidoreductase (BH4/BH2) mediated eNOS uncoupling resulting in (1) decreased nitric oxide production (NO), (2) increased superoxide radical ($O_2^{\bullet -}$) and (3) peroxynitrite anion (ONOO−). The effect of introducing oxidative B(a)P-metabolites into this cycle upregulates the expression of the BH4/BH2 oxidoreductase as was empirically determined in Fig. 5. These three scenarios are proposed to lead to the apparent later-life (P53) uncoupling of eNOS as a result of high oxidative cardiovascular tissue burdens during early-life, developmental processes.

Table 1

Primers used in real-time quantitative RT-PCR experiment.

Name	Symbol	Primer	Sequence
Angiotensin	AngII	Forward	CTGTGAAGGAGGGAGACTGC
Angiotensin	AngII	Reverse	GTGGACTGTAGCAGGGGTGT
Neuronal nitric oxide synthase	NOS1	Forward	CTGCAAAGCCCTAAGTCCAG
Neuronal nitric oxide synthase	NOS1	Reverse	AGCAGTGTTCCTCTCCTCCA
Endothelial nitric oxide synthase	NOS3	Forward	TGACCCTCACCGATACAACA
Endothelial nitric oxide synthase	NOS3	Reverse	CTGTACAGCACAGCCACGTT
7,8-Dihydrobiopterin oxidoreductase	Spr	Forward	TACAGCCCATCTCTGAGTGC
7,8-Dihydrobiopterin oxidoreductase	Spr	Reverse	CTTCATAATGGCCTCCTCCA

Three genes known to be involved in blood pressure regulation (AngII, eNOS, iNOS and BH4/BH2 oxidoreductase) were selected to be measured by qRT-PCR. Primers shown in Table 1 were designed using OligoPerfect Designer Software (Invitrogen, USA).

Table 2

Average number of offspring born per litter.

Animal dose group	Dams	Number of pups/l
Vehicle – Control	17	10 ± 0.32
150 μg/kg BW	7	12 ± 0.65
300 μg/kg BW	6	11 ± 0.80
600 μg/kg BW	15	12 ± 0.53
1200 μg/kg BW	9	11 ± 0.59

Offspring exposed *in utero* to B(a)P exhibit no overt signs of toxicity effects on litter size. As shown in Table 2, there was no significant difference between the average number of pups born per litter for control or B(a)P exposed litters.

Table 3A

KEGG molecular pathway enrichment analysis of gene expression changes from control P53 versus 1200 μg/kg BW B(a)P-exposed offspring heart tissue transcriptome data set.

KEGG enriched pathway	Observed [O]	Expected [E]	Enrichment [R] = [O]/[E]	Raw *p*-value	BH adjusted *p*-value
PPAR signaling pathway	6	0.40	14.88	3.31E–06	1.00E–04
Renin-angiotensin system	2	0.11	18.35	5.30E–03	2.13E–02
Hematopoietic cell lineage	5	0.42	11.91	6.58E–05	1.10E–03
Drug metabolism by CYP_{P450}	4	0.45	8.84	1.10E–03	9.40E–03
Tight junction	5	0.73	6.85	9.00E–04	9.40E–03
Cell adhesion molecules-CAMs	5	0.86	5.84	1.70E–03	1.16E–02
Primary bile acid biosynthesis	2	0.08	24.46	3.00E–03	1.70E–02
Retinol metabolism	3	0.38	7.98	6.40E–03	2.13E–02
Metabolism of xenobiotics by CYP_{P450}	3	0.39	7.75	6.90E–03	2.13E–02

Enrichment analysis from control P 53 *versus* 1200 μg/kg BW transcriptome data set. Column 1 – Significantly enriched KEGG pathway. Column 2 – Enrichment ratio (R) derived by ratio of significantly altered genes mapping to the pathway *versus* expected number of genes mapping to pathway form a reference baseline database. Column 3 – raw enrichment *p*-value of hypergeometic test for enrichment. Column 4 – Benjamini and Hochburg adjusted *p*-value to correct for multiple testing.

Table 3B

Cardiovascular endpoints minitored in control and *in utero* B(a)P-exposed offspring

LEH rats	Heart rate (bmp)	Systolic pressure (mmHg)	Diostolic pressure (mmHg)
Control	504.6 ± 15.7	131.6 ± 1.2	85.0 ± 4.2
600 μg/kg	554.6 ± 26.2 *	156.1 ± 45 *	113.0 ± 3.3 *
1200 μg/kg	466.3 ± 16.9 *	200.4 ± 2.4 *	155.6 ± 3.2 *

* $p < 0.05$.

Table 4

(A) Genes found to be modulated subsequent to *in utero* B(a)P exposure in rat offspring. Expression fold changes of genes in "regulation of blood pressure" gene ontology biological process (GO:008217) are shown as well as the REFSEQ-mRNA accession number; (B) genes found not to be modulated subsequent to *in utero* B(a)P exposure in rat offspring.

REFSEQ-mRNA	Fold Change	Gene Symbol	Gene Name
A			
NM_004797	8.9	Adipoq	Adiponectin, C1Q and collagen domain
NM_000029.3	8.5	AngII	Angiotensinogen (serpin peptidase inhibitor clade A, member 8)
NM_000025	9.3	Adrb3	Adrenergic, beta-3-, receptor
NM_001058.3	9.9	Tacr1	Tachykinin receptor 1
NM_138712	5.8	PPARγ	Peroxisome proliferator-activated receptor
NM_001057	−2.2	Tac2	Tachykinin 2
Gene symbol	Gene name		
B			
ADAMTS18	ADAM metallopeptidase with thrombospondin type 1 motif 18		
AGTR2	Angiotensin II receptor, type 2		
GPD1	Glycerol-3-phosphate dehydrogenase 1 (soluble)		
HRASLS5	HRAS-like suppressor family, member 5		
Tac4	Tachykinin receptor 4		
Tacr2	Tachykinin receptor 2		
Tacr3	Tachykinin receptor 3		
TF	Transferrin		
TFF2	Trefoil factor 2		
THRSP	Thyroid hormone responsive protein, isoform CRA_a		

Gene ontology biological process analysis of gene expression from control P 53 *versus* 1200 μg/kg BW transcriptome data set. Column 1 – REFSEQ mRNA number. Column 2 – Fold change. Column 3 – Gene symbol. Column 4 – Gene name.